Electronic Supplementary Information

Experimental section

Materials: Ammonium molybdate tetrahydrate ($(NH_4)_6Mo_7O_{24}\cdot4H_2O$), glucose monohydrate ($C_6H_{12}O_6$), carbon cloth, anhydrous ethanol (C_2H_6O), graphene oxide dispersion (GO), Nafion solution, sodium nitrite ($NaNO_2$), anhydrous sodium sulfate (Na_2SO_4) sodium citrate dihydrate ($C_6H_5Na_3O_7\cdot2H_2O$) Nafion solution, ammonium chloride (NH_4Cl), sodium hydroxide (NaOH), ferro-nitrocyanide dihydrate ($C_5FeN_6Na_2O\cdot2H_2O$), salicylic acid ($C_7H_6O_3$), sodium hypochlorite solution (NaClO), and p-dimethylaminobenzaldehyde ($C_9H_{11}NO$) can be used directly without any additional treatment.

Preparation of MoO_2@C/RGO and MoO_2/RGO: 0.1 g $(NH_4)_6Mo_7O_{24}\cdot4H_2O$ and 0.0275 g glucose were dissolved in 25 mL deionized water and then mixed with 4 mL GO solution (5 mg/mL) and sonicated for 30 min. The mixture was transferred into a 50 mL PTFE-lined stainless-steel autoclave and heated in an oven at 180 °C for 12 h. The product was extracted by centrifugation at 10,000 rpm for 10 min, which was then washed repeatedly with deionized water and finally dried by lyophilization. The samples were then heated at 800 °C for 4 h under an argon atmosphere with a heating rate of 5 °C min^{-1} to obtain the MoO_2@C/RGO. The samples prepared without adding glucose according to the above steps were denoted as MoO_2/RGO.

Working electrode preparation: For the preparation of the working electrode, 2 mg of catalyst was dispersed in a mixed solution containing 480 μL ethanol, 480 μL deionised water, and 40 μL of Nafion solution (5 wt%). The mixture was sonicated for 1 h to form a homogeneous catalyst ink. 50 μL of the resulting catalyst ink was drop-cast onto a carbon cloth (0.25 cm^2) and the final mass loading was calculated to be 0.4 mg cm^{-2}.

Characterization: XRD data were determined using X-ray diffractometer with Cu Kα radiation (DX-2700B). SEM measurements were carried out on a field-emission scanning electron microscopy (FEI Insect F50). TEM images were obtained using an atomic-resolution scanning transmission electron microscopy (FEI Talos F200S Super). XPS measurements were performed with Thermo Fischer ESCALAB Xi^+. The absorbance data were measured by an ultraviolet-visible spectrophotometer.

Electrochemical measurements: All electrochemical measurements were carried out in an H-shaped electrochemical cell separated by a Nafion membrane using CHI 660E electrochemical workstation (Chenhua, Shanghai). MoO_2@C/RGO, Ag/AgCl, and graphite rod were used as working electrode, reference electrode, and reference electrode, respectively. The area of the working electrode immerse in electrolyte is 0.25 cm^2. LSV was performed in Ar-saturated 0.5 M Na_2SO_4 with 0.1 M $NaNO_2$ at a scan rate of 5 mV s^{-1}. All potentials reported in this work were converted to reversible hydrogen electrode (RHE) scale and current densities were normalized to the geometric surface area.

Determination of NH_3: The NH_3 concentration in the solution was determined (the obtained electrolyte was diluted 50 times) by the indophenol blue method. In detail, 2 mL of coloring solution (1 M NaOH containing 5% salicylic acid and 5% sodium citrate), 1 mL of oxidizing solution (0.05 M NaClO), and 0.2 mL of catalyst solution

(1 wt% $C_5FeN_6Na_2O\cdot 2H_2O$) were added to 2 mL of the electrolyte after electrolysis. After standing for 2 h in the dark, the UV-Vis absorption spectra were measured. The concentration of NH_3 was identified using absorbance at a wavelength of 655 nm. The concentration-absorbance curve was calibrated using the standard NH_4Cl solution with known concentrations of 0, 0.25, 0.5, 1.0, 1.5, 2.0 and 2.5 μg mL^{-1} in 0.5 M Na_2SO_4. The fitting curve ($y = 0.47264x + 0.0255$, $R^2 = 0.9997$) shows good linear relation of absorbance value with NH_3 concentration.

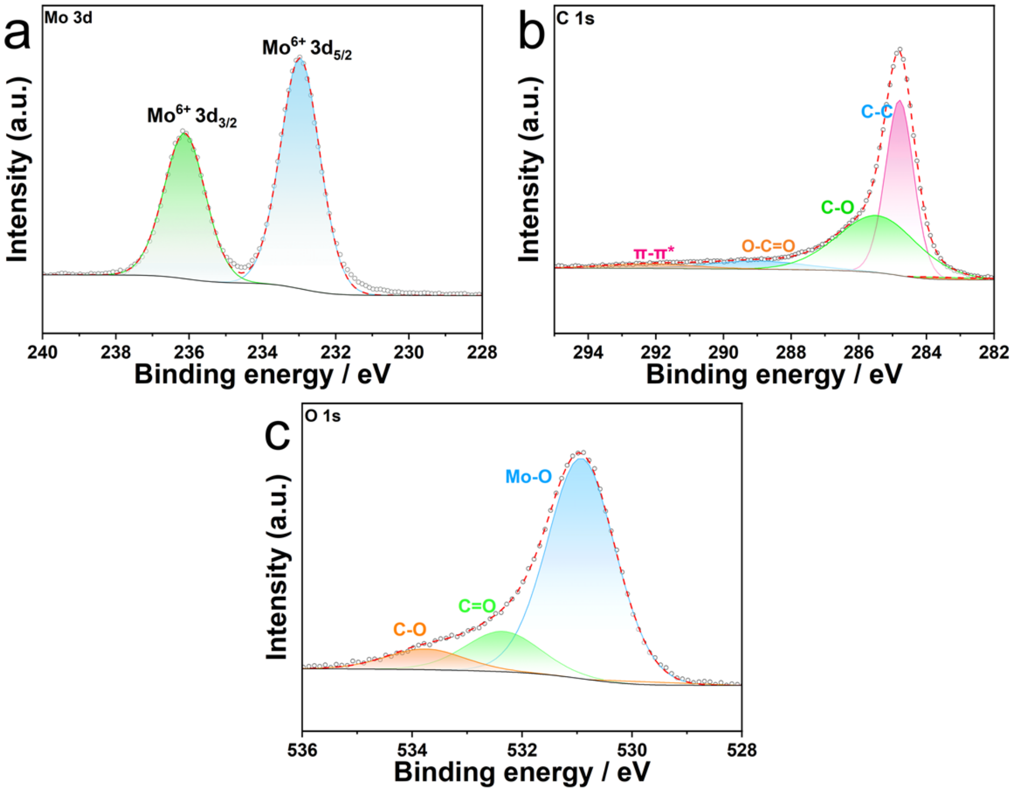

Fig. S1 XPS spectra for MoO$_2$/RGO in the (a) Mo 3d, (b) C 1s, and (c) O 1s regions.

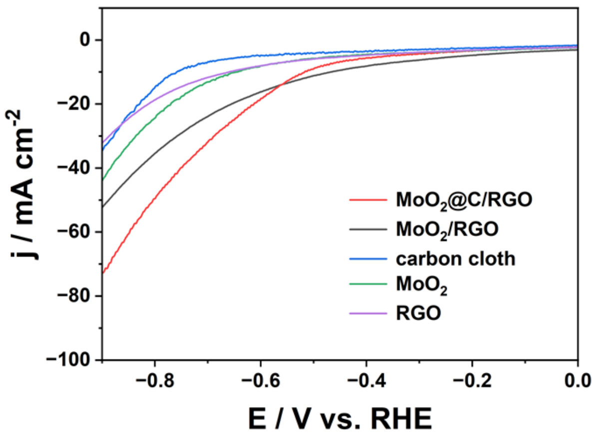

Fig. S2 The LSV curves of MoO_2@C/RGO, MoO_2/RGO, carbon cloth, MoO_2, and RGO in 0.5 M Na_2SO_4 with 0.1 M $NaNO_2$.

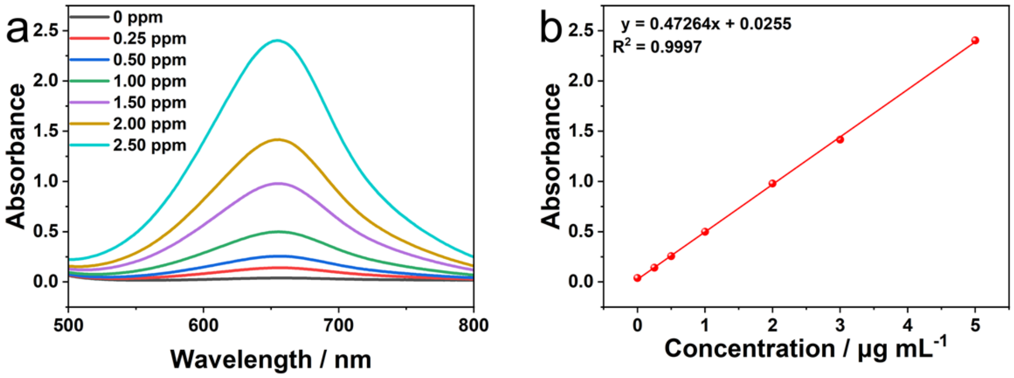

Fig. S3 (a) UV-V is spectra and (b) corresponding calibration curve used for calculation of NH_4^+ concentration.

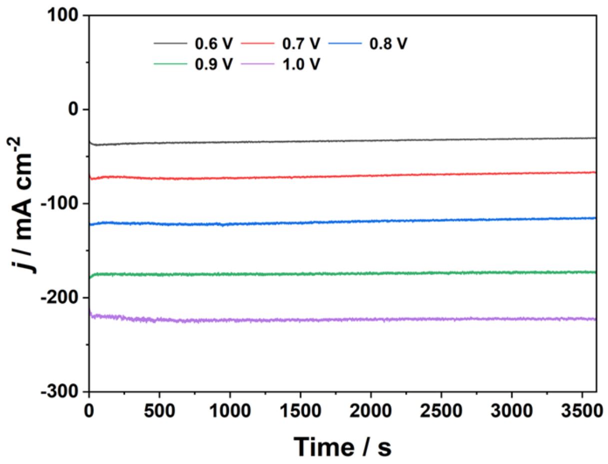

Fig. S4 Chronoamperometric curve of MoO_2@C/RGO for NO_2^-RR at various potentials.

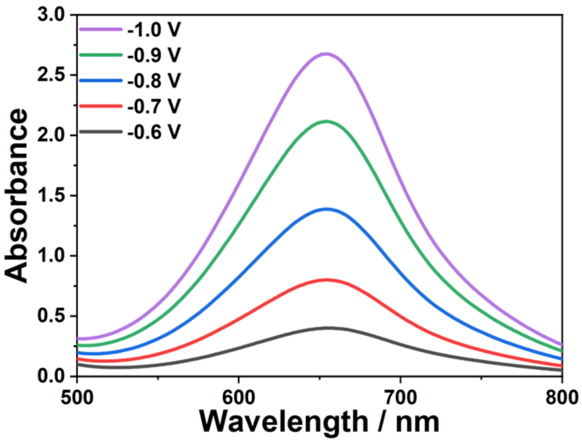

Fig. S5 UV-Vis absorption spectra of NH_4^+ production by MoO_2@C/RGO at different potentials.

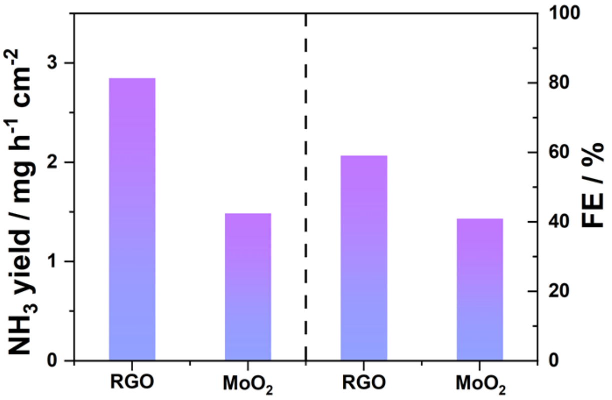

Fig. S6 NH_3 yields and FEs of MoO_2 and RGO at -0.9 V.

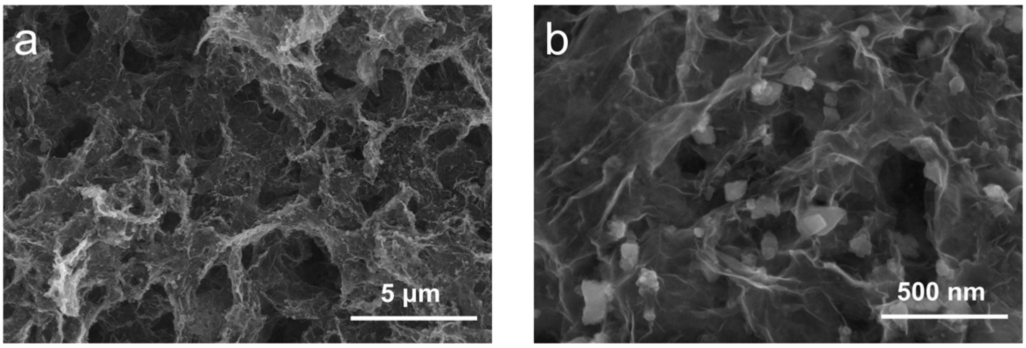

Fig. S7 SEM images of MoO_2/RGO.

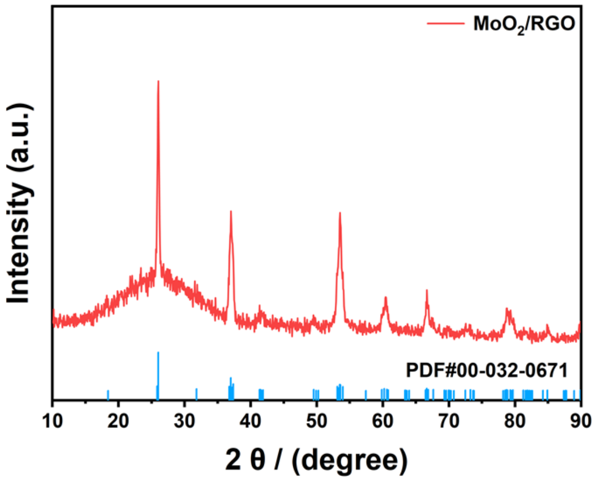

Fig. S8 XRD pattern for MoO$_2$/RGO.

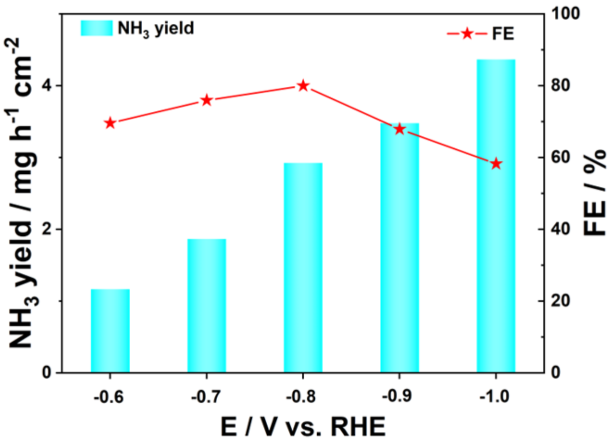

Fig. S9 NH_3 yields and FEs of MoO_2/RGO at different potentials.

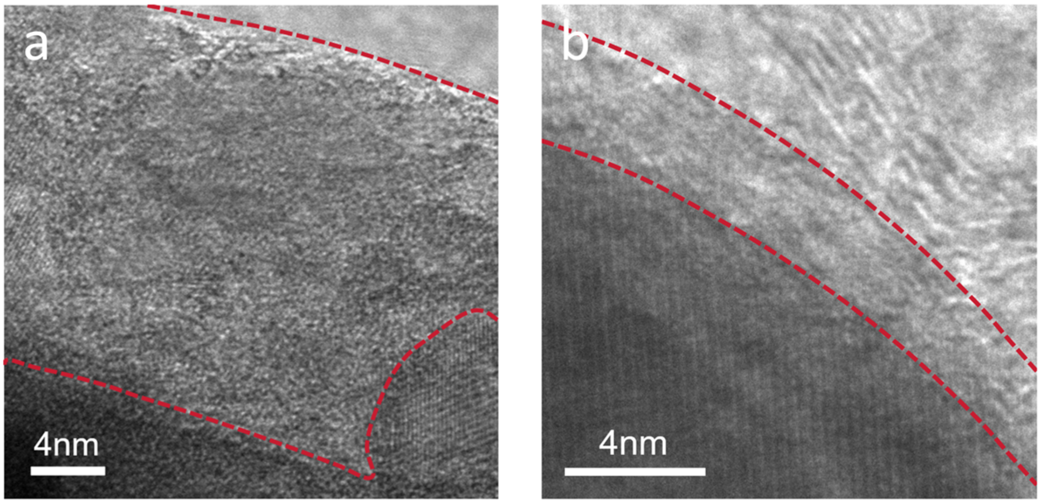

Fig. S10 HRTEM images of MoO_2@C/RGO prepared with different glucose contents:

(a) 0.0367 g, (b) 0.0138 g.

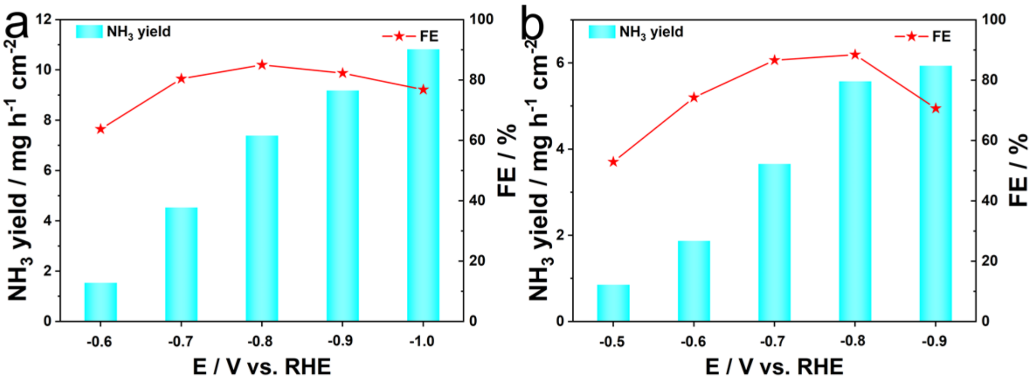

Fig. S11 NH_3 yields and FEs of MoO_2@C/RGO prepared with different glucose contents: (a) 0.0367 g, (b) 0.0138 g.

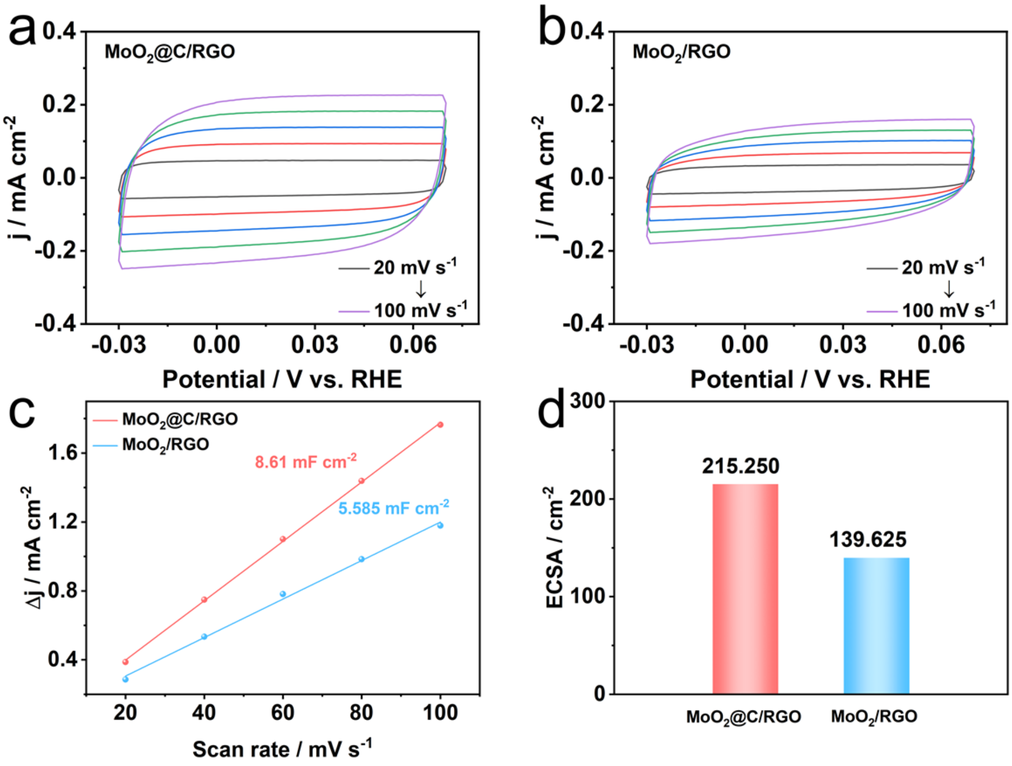

Fig. S12 CV curves of (a) MoO$_2$@C/RGO and (b) MoO$_2$@C/RGO. (c) C$_{dl}$ and (d) ECSA of MoO$_2$@C/RGO and MoO$_2$/RGO.

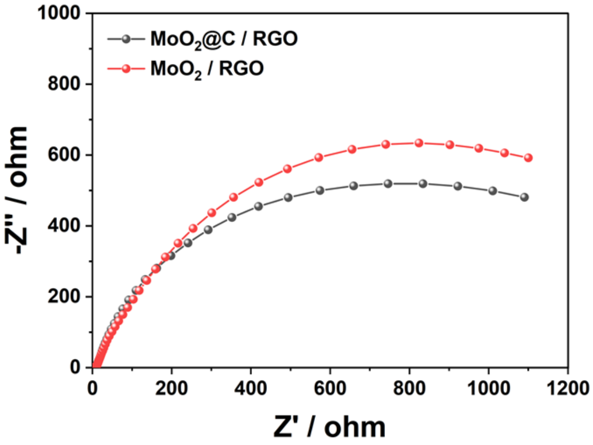

Fig. S13 EIS patterns of MoO_2@C/RGO and MoO_2/RGO.

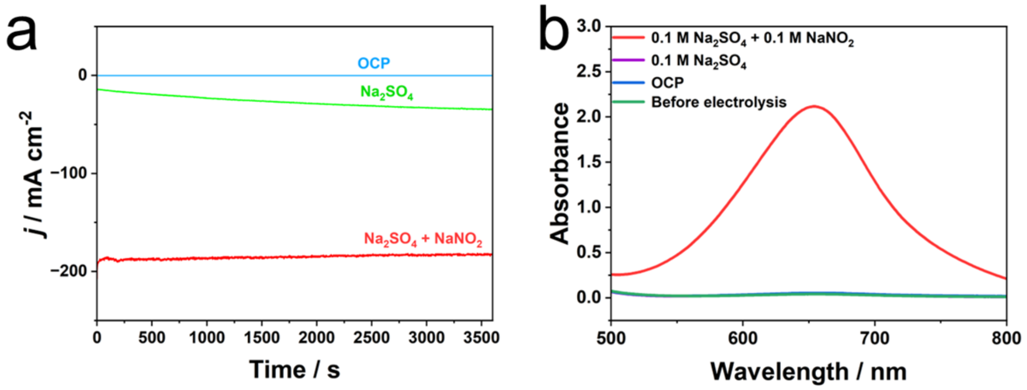

Fig. S14 (a) Chronometric current curves of MoO_2@C/RGO in different experimental conditions. (b) UV-Vis absorption spectra of NH_3 production under different experimental conditions.

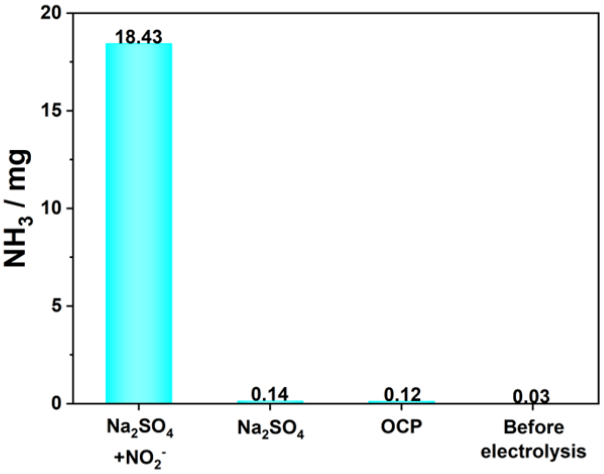

Fig. S15 NO_2^-RR performance of MoO_2@C/RGO under different experimental conditions.

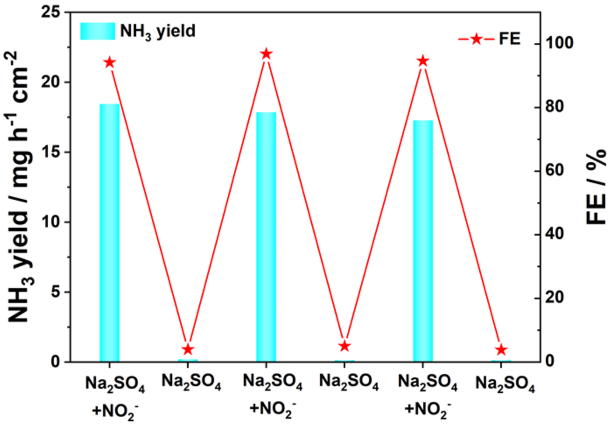

Fig. S16 NH_3 yield and FE of MoO_2@C/RGO evaluated by alternating cycling experiments.

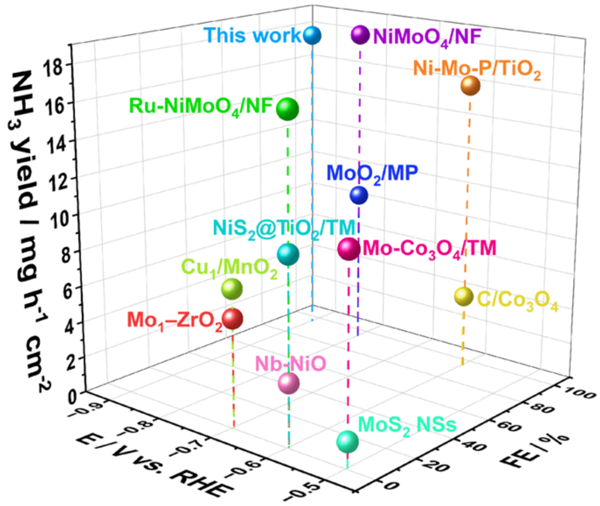

Fig. S17 Comparison of the electrochemical performance with some reported catalysts (detailed information available in Table S1).

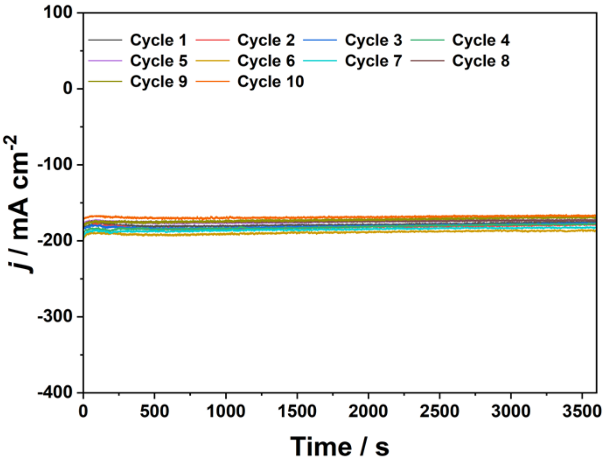

Fig. S18 Chronoamperometry curves of MoO_2@C/RGO for cycling tests in 0.5 M Na_2SO_4 with 0.1 M NO_2^- at −0.9 V.

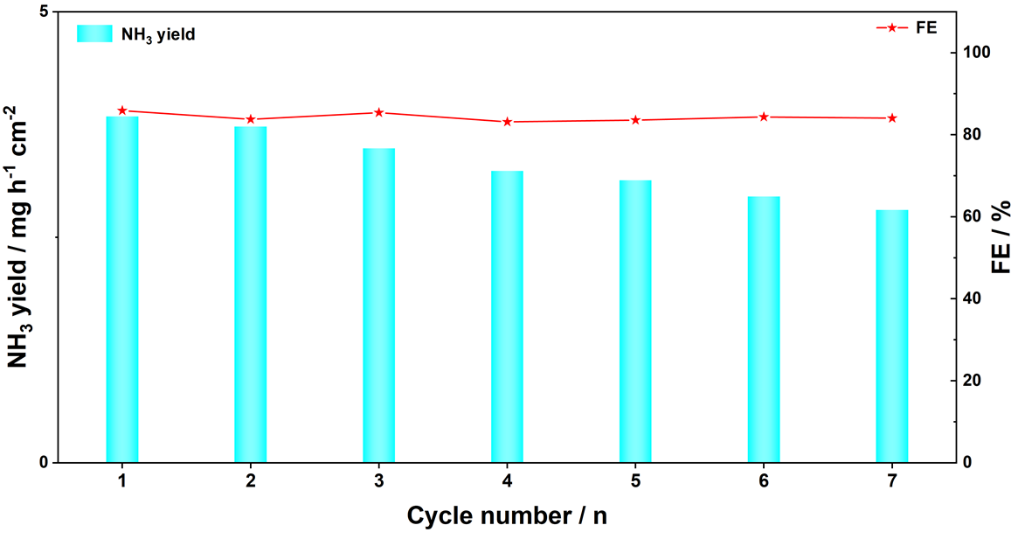

Fig. S19 NO_2^-RR performance of MoO_2/RGO in cycling experiments.

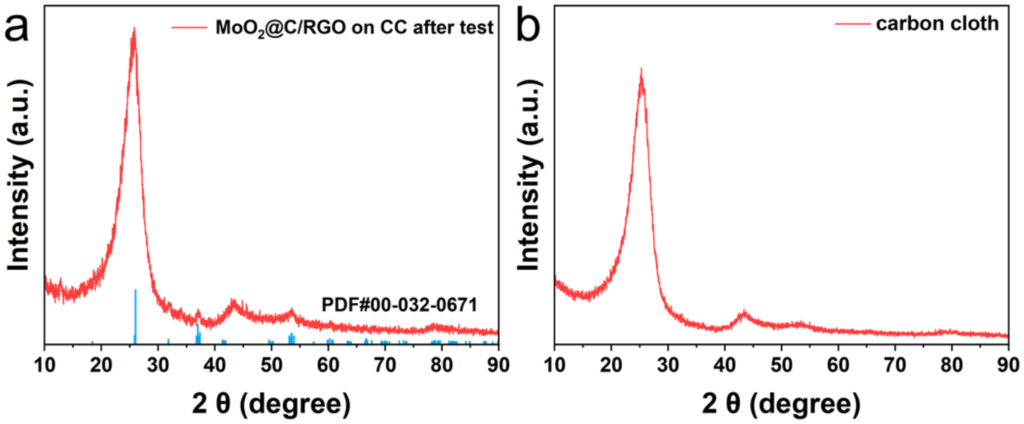

Fig. S20 XRD pattern of (a) MoO_2@C/RGO on carbon cloth after cycling tests and (b) carbon cloth. In Fig. S20a, the broad peaks at 25.3 and 43.4 belong to the carbon cloth substrate.

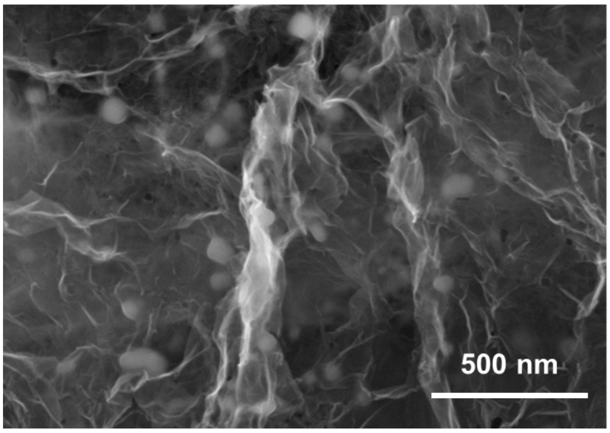

Fig. S21 SEM image of the MoO_2@C/RGO after cycling tests.

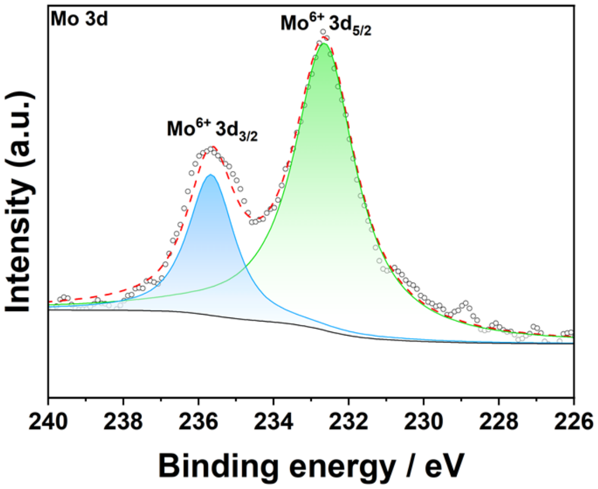

Fig. S22 Mo 3d XPS spectra of MoO_2@C/RGO after cycling tests.

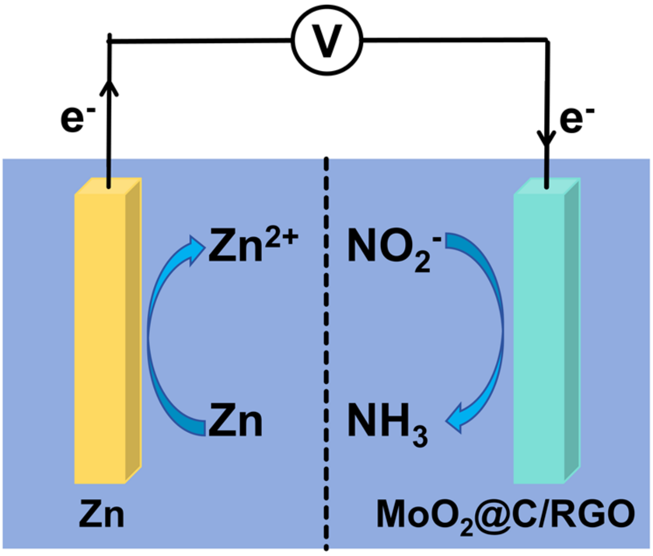

Fig. S23 The demonstration figure of the aqueous Zn−NO_2^- battery.

Table S1 Comparison the catalytic performance of MoO_2@C/RGO with other reported NO_2^-RR electrocatalysts.

Catalyst	Electrolyte	NH_3 yield rate (mg h^{-1} cm^{-2})	FE (%)	Ref.
MoO_2@C/RGO	**0.5 M Na_2SO_4 + 0.1 M NO_2^-**	**17.64**	**95.79**	**This work**
Ni-Mo-P/TiO_2	0.1 M NaOH + 0.1 M NO_2^-	16.12	95.6	1
C/Co_3O_4	0.5 M K_2SO_4 + 0.05 mM NO_2^-	4.1	95.1	2
Cu_1/MnO_2	0.5 M Na_2SO_4 + 0.1 M NO_2^-	7.48	93.3	3
NiS_2@TiO_2/TM	0.1 M NaOH + 0.1 M NO_2^-	10.06	92.1	4
Ru-$NiMoO_4$/NF	0.5 M Na_2SO_4 + 0.1 M NO_2^-	17.19	95.56	5
MoS_2 NSs	0.5 M Na_2SO_4 + 0.1 M NO_2^-	1.37	93.52	6
Mo_1-ZrO_2	0.5 M Na_2SO_4 + 0.1 M NO_2^-	5.90	94.83	7
Nb-NiO	0.5 M Na_2SO_4 + 0.1 M NO_2^-	3.41	92.4	8
MoO_2/MP	0.5 M Na_2SO_4 + 0.1 M NO_2^-	8.68	94.5	9
$NiMoO_4$/NF	0.5 M Na_2SO_4 + 0.1 M NO_2^-	18.10	94.49	10
Mo-Co_3O_4/TM	0.1 M NaOH + 0.1 M NO_2^-	11.08	96.9	11
Mn_1/MoO_{3-x}	0.5 M Na_2SO_4 + 0.5 M NO_2^-	9.29	92.6	12
am-MoO_3	0.5 M Na_2SO_4 + 0.1 M $NaNO_2$	7.21	94.8	13
Cu_1/Mo_2C	0.5 M Na_2SO_4 + 0.1 M NO_2^-	8.04	91.5	14
$MoSe_{2-x}$/CC	0.1 M PO_4^{3-} + 0.1 M NO_2^-	7.58	96.9	15
Au@CC-SDS	0.1 M PO_4^{3-} + 0.1 M NO_2^-	1.25	80.7	16

References

1. Z. Ren, Q. Chen, J. Zhang, X. An, Q. Liu, L. Xie, W. Yao, X. Sun and Q. Kong, *Mater. Today Phy.*, 2023, **36**, 101162.
2. R. Zhang, S. Zhang, Y. Guo, C. Li, J. Liu, Z. Huang, Y. Zhao, Y. Li and C. Zhi, *Energy Environ. Sci.*, 2022, **15**, 3024−3032.
3. Y. Wan, W. Du, K. Chen, N. Zhang and K. Chu, *J. Colloid Interf. Sci.*, 2023, **652**, 2180−2185.
4. X. He, L. Hu, L. Xie, Z. Li, J. Chen, X. Li, J. Li, L. Zhang, X. Fang, D. Zheng, S. Sun, J. Zhang, A. Ali Alshehri, Y. Luo, Q. Liu, Y. Wang and X. Sun, *J. Colloid Interf. Sci.*, 2023, **634**, 86−92.
5. G. Wang, Q. Chen, J. Zhang, X. An, Q. Liu, L. Xie, W. Yao, X. Sun and Q. Kong, *J. Colloid Interf. Sci.*, 2024, **661**, 401−408.
6. L. Yi, P. Shao, H. Li, M. Zhang, X. Peng, K. Chen, X. Liu and Z. Wen, *J. Power Sources*, 2023, **559**, 232668.
7. W. Du, Y. Zhang, K. Chen, G. Zhang and K. Chu, *J. Clean. Prod.*, 2023, **424**, 138875.
8. Y. Zhang, Y. Wan, X. Liu, K. Chen and K. Chu, *iScience*, 2023, **26**, 107944.
9. G. Wang, Q. Chen, X. An, Q. Liu, L. Xie, J. Zhang, W. Yao, X. Liu, S. Sun, X. Sun and Q. Kong, *Colloid. Surf. A*, 2023, **657**, 130549.
10. G. Wang, Q. Chen, J. Zhang, X. An, Q. Liu, L. Xie, W. Yao, X. Sun and Q. Kong, *J. Colloid Interf. Sci.*, 2023, **647**, 73−80.
11. Y. Li, L. Ouyang, J. Chen, X. Fan, H. Sun, X. He, D. Zheng, S. Sun, Y. Luo, Q. Liu, L. Li, W. Chu, J. Du, Q. Kong, B. Zheng and X. Sun, *J. Colloid Interf. Sci.*, 2024, **663**, 405−412.
12. Z. Zhang, Y. Wan, S. Shang, Z. Li and K. Chu, *Fuel*, 2025, **381**, 133394.
13. T. Wu, F. Zhang, J. Wang, X. Liu, Y. Tian and K. Chu, *Dalton Trans.*, 2024, **53**, 877-881.
14. G. Wang, R. Ma, N. Zhang, Y. Guo and K. Chu, *Chem. Commun.*, 2023, **59**, 13887-13890.
15. L. Hu, X. He, J. Yao, X. Li, J. Chen, J. Li, X. Fan, L. Xie, Z. Cai, S. Sun, D. Zheng, B. Ying, Y. Wang, Y. Luo, Q. Liu, A. Farouk, M. S. Hamdy, S. Alfaifi, Y. Liao, Q. Kong and X. Sun, *Mater. Today Phy.*, 2023, **36**, 101170.
16. W. Zhang, T. Wang, X. Xing, H. Yin, J. Li, W. Xiong and H. Li, *ACS Sustainable Chem. Eng.*, 2024, **12**, 10313-10324.